

N doping of $\text{TiO}_2(110)$: Photoemission and density-functional studies

Cite as: J. Chem. Phys. **125**, 094706 (2006); <https://doi.org/10.1063/1.2345062>

Submitted: 17 May 2006 . Accepted: 01 August 2006 . Published Online: 01 September 2006

A. Nambu, J. Graciani, J. A. Rodriguez, Q. Wu, E. Fujita, and J. Fdez Sanz



View Online



Export Citation

ARTICLES YOU MAY BE INTERESTED IN

[Titanium nitride oxidation chemistry: An x-ray photoelectron spectroscopy study](#)
Journal of Applied Physics **72**, 3072 (1992); <https://doi.org/10.1063/1.351465>

[Electronic properties of N- and C-doped \$\text{TiO}_2\$](#)
Applied Physics Letters **87**, 011904 (2005); <https://doi.org/10.1063/1.1991982>

[Deep-level optical spectroscopy investigation of N-doped \$\text{TiO}_2\$ films](#)
Applied Physics Letters **86**, 132104 (2005); <https://doi.org/10.1063/1.1896450>

Lock-in Amplifiers
up to 600 MHz



N doping of TiO₂(110): Photoemission and density-functional studies

A. Nambu, J. Graciani,^{a)} J. A. Rodriguez,^{b)} Q. Wu, and E. Fujita
 Chemistry Department, Brookhaven National Laboratory, Upton, New York 11973

J. Fdez Sanz
 Departamento de Química Física, Universidad de Sevilla, E-41012 Sevilla, Spain

(Received 17 May 2006; accepted 1 August 2006; published online 1 September 2006)

The electronic properties of N-doped rutile TiO₂(110) have been investigated using synchrotron-based photoemission and density-functional calculations. The doping via N₂⁺ ion bombardment leads to the implantation of N atoms (~5% saturation concentration) that coexist with O vacancies. Ti 2*p* core level spectra show the formation of Ti³⁺ and a second partially reduced Ti species with oxidation states between +4 and +3. The valence region of the TiO_{2-x}N_y(110) systems exhibits a broad peak for Ti³⁺ near the Fermi level and N-induced features above the O 2*p* valence band that shift the edge up by ~0.5 eV. The magnitude of this shift is consistent with the “redshift” observed in the ultraviolet spectrum of N-doped TiO₂. The experimental and theoretical results show the existence of attractive interactions between the dopant and O vacancies. First, the presence of N embedded in the surface layer reduces the formation energy of O vacancies. Second, the existence of O vacancies stabilizes the N impurities with respect to N₂(*g*) formation. When oxygen vacancies and N impurities are together there is an electron transfer from the higher energy 3*d* band of Ti³⁺ to the lower energy 2*p* band of the N²⁻ impurities. © 2006 American Institute of Physics.
 [DOI: 10.1063/1.2345062]

I. INTRODUCTION

Photochemical water splitting to H₂ and O₂ has been successfully carried out using ultraviolet irradiation of aqueous suspensions (or thin-film photoanodes) of various photocatalysts including TiO₂,¹ transition-metal doped TiO₂,^{2,3} SrTiO₃,⁴ and transition-metal loaded SrTiO₃.⁵ Among these photocatalysts, TiO₂ is the one most frequently employed because of its low cost, nontoxicity, and structural stability.² However, pure titania is only activated by ultraviolet light.¹ Recently, N-doped titania (TiO_{2-x}N_y) has been synthesized and used as a photocatalyst that utilizes visible light (>420 nm).⁶⁻⁸ This material absorbs solar light in a region where TiO₂ or SrTiO₃ does not due to their wide band gaps. Such a behavior is very important for practical applications since solar light contains less than 5% of ultraviolet radiation. In principle, a dopant element can induce energy levels within the band gap of TiO₂ that may increase the yield for electron-hole pair formation under illumination with visible light.^{1,2,6} Two different models have been proposed to explain the good performance of TiO_{2-x}N_y as a photocatalyst.^{6,9,10} In one model, hybridization of the N 2*p* states of the dopant with the O 2*p* valence band of TiO₂ leads to band narrowing.⁶ Optical absorption studies on N-doped TiO₂ point to a gap narrowing,⁶ but no band gap narrowing has been observed in photoemission studies.¹¹ In

the second model, the dopant N 2*p* levels form localized states within the band gap just above the O 2*p* valence band maximum for titania.^{9,10}

In a recent study the effects of N doping on the electronic and structural properties of TiO₂ rutile (110) and anatase (101) single crystals were investigated using photoemission and scanning tunneling microscopy (STM).¹¹ The oxide surfaces were doped using low energy (1 keV) N ion implantation. It was found that N is probably present in a N³⁻ valence state, which facilitates the formation of oxygen vacancies and Ti 3*d* band gap states at elevated temperatures. The increased O vacancy formation triggers a massive 1 × 2 reconstruction of the rutile (110) surface,¹¹ although the N concentration is relatively low (~3%). The fundamental causes for this phenomenon are not well understood. In general, the positions preferred by the N atoms in the lattice of an oxide surface are not known or why it is so difficult to obtain large concentrations of the dopant via N ion implantation or through chemical reaction with NH₃ or NO_x species.¹²⁻¹⁴ For example, *in situ* measurements of time-resolved x-ray diffraction for the interaction of NH₃ with titania at elevated temperatures (600–750 °C) show a direct conversion of the oxide into TiN and the amount of N incorporated into the titania lattice is very small (≲5%).¹⁵

In this article we use synchrotron-based photoemission and density-functional (DF) calculations to examine N doping of TiO₂(110). The doping via N₂⁺ ion bombardment leads to the implantation of N atoms that coexist with O vacancies. The presence of O vacancies is necessary to stabilize the embedded N and avoid the formation of N₂ gas. When oxygen vacancies and N impurities are together there is an electron transfer from the higher energy 3*d* band of Ti³⁺ to the

^{a)}Permanent address: Departamento de Química Física, Universidad de Sevilla, Spain.

^{b)}Author to whom correspondence should be addressed. Electronic mail: rodriguez@bnl.gov

lower energy $2p$ band of the N^{2-} impurities. The valence region of the N-doped $TiO_2(110)$ systems exhibits a broad peak for Ti^{3+} near the Fermi level and N-induced features above the O $2p$ valence band that shift the edge up by ~ 0.5 eV. The magnitude of this shift is consistent with the “redshift” observed in the ultraviolet spectrum of N-doped TiO_2 .

II. EXPERIMENTAL AND THEORETICAL METHODS

A. Photoemission studies

All the experiments were performed at beamline U7A of the National Synchrotron Light Source (NSLS) in Brookhaven National Laboratory. The end station was equipped with a hemispherical electron-energy analyzer, an ion gun, a quadrupole mass spectrometer, and several variable leak valves for the dosing of gases. The sample holder has been described previously.¹² The rutile $TiO_2(110)$ single crystal was wrapped by a Ta foil to prevent charging and an 8 mm diameter area was exposed to synchrotron irradiation. The temperature of the substrate was monitored by a thermocouple (type C) welded to the Ta foil and could vary from 100 to 1400 K by liquid nitrogen cooling and either electron bombardment and/or direct resistive heating. The uncertainty in the temperature measurements was ± 5 K. The base pressure of the end station was $\sim 1 \times 10^{-9}$ torr. A photon energy of 625.0 eV was employed to acquire the core level (O $1s$, Ti $2p$, N $1s$) spectra,¹² while 325.0 eV was used for the valence band measurements.

The sample was cleaned by cycles of Ar^+ ion sputtering and 900 K annealing in 1×10^{-6} torr of O_2 followed by cooling under the same partial pressure of O_2 .¹² This cleaning procedure was repeated until no carbon (or other) contamination was observed by photoemission. In this paper, the clean sample is referred to as “stoichiometric $TiO_2(110)$,” although it may contain a small amount of O vacancies (density of 5%–7%).¹² The nitrogen doped samples were prepared by N_2^+ ion implantation with a 3 keV ion acceleration energy under a 1×10^{-6} torr of N_2 back pressure using a conventional ion gun. The average sample leak current during ion irradiation was $\sim 4 \mu A$ and the estimated total amount of irradiated N_2 molecules was $\sim 10^{17}$ ions/cm². For comparison, Ar^+ bombarded $TiO_2(110)$ surfaces were prepared following the same procedure but replacing N_2^+ ions by Ar^+ ions. The purity (99.999%) of the implanted ion gasses (N_2 or Ar) was checked by a mass spectrometer, and the concentration of impurities in the oxide sample was below the detection limit of photoemission (< 0.02 ML). After these ion treatments, the sample was kept in ultrahigh vacuum (UHV) at 900 K for 2 h. An earlier study¹⁶ reported that N-doped films prepared with pure N_2^+ ions lead to thermally unstable doped nitrogen; however, in our experiments, even with pure N_2^+ , the prepared N-doped TiO_2 was stable under thermal treatment. At least after 2 h aging at 900 K in UHV, we could observe nitrogen on the sample by photoemission.

B. Density functional calculations

In order to model the $TiO_{2-x}N_x(110)$ surfaces, periodic DF calculations were carried out using the VASP 4.6 code^{17,18} and ultrasoft pseudopotentials.¹⁹ In these calculations energy was obtained using the generalized gradient approximation (GGA) implementation of DF theory proposed by Perdew *et al.*²⁰ and the electronic states were expanded using plane waves as a basis set with a cutoff of 396 eV. The number of k points used was generated using the Monkhorst-Pack method²¹ and the grid was $4 \times 2 \times 1$. To obtain faster convergence with respect to the number of k points a Gaussian smearing method²² was used as step function for the partial occupancies.

Forces on the ions were calculated through the Hellmann-Feynman theorem as the partial derivatives of the free energy with respect to the atomic position, including the Harris-Foulkes²³ correction to forces. This calculation of the forces allows a geometry optimization using the conjugate-gradient scheme. Iterative relaxation of atomic positions was stopped when the change in all forces was smaller than 0.01 eV/Å.

The (110) surface of rutile was modeled with a three-layer slab (nine atomic layers) separated by a vacuum of 15 Å. The atomic coordinates of the bottom layer were fixed at the optimized bulk positions and the other two layers were fully relaxed. This model for the $TiO_2(110)$ surface has been used successfully.^{24,25} We have compared our energies for formation of O vacancies in several lattice sites (bridging, in plane, subsurface) with those obtained by Oviedo *et al.*²⁶ for a fully relaxed five layers model. They are in very good agreement (differences < 0.2 eV). Thus, the model used is good enough to describe the $TiO_2(110)$ surface.

In Sec. III, we report the energetics for the formation of O vacancies in titania, the embedding of N into the oxide lattice, and the interaction between the dopant element and O vacancies. The formation energy for an oxygen vacancy was calculated as follows:

$$E(V_O) = \frac{1}{2}E(\text{gaseous } O_2 \text{ molecule}) + E(\text{surface with } V) - E(\text{perfect surface}). \quad (1)$$

The adsorption energy of a N atom on a perfect surface,

$$E(N \text{ ads}) = E(\text{ads-N surface}) - E(N \text{ atom}) - E(\text{perfect surface}), \quad (2)$$

or on a surface with O vacancies,

$$E(N \text{ ads}) = E(\text{ads-N surface}) - E(N \text{ atom}) - E(\text{surface with } V). \quad (3)$$

The stability of a structural N impurity with respect to $N_2(g)$ formation leaving an oxygen vacancy in the system was given by

$$E(N_2 \text{ formation}) = \frac{1}{2}E(\text{gaseous } N_2) + E(\text{surface with } V) - E(\text{implanted-N surface}). \quad (4)$$

And finally, the stability of an adsorbed or interstitial N im-

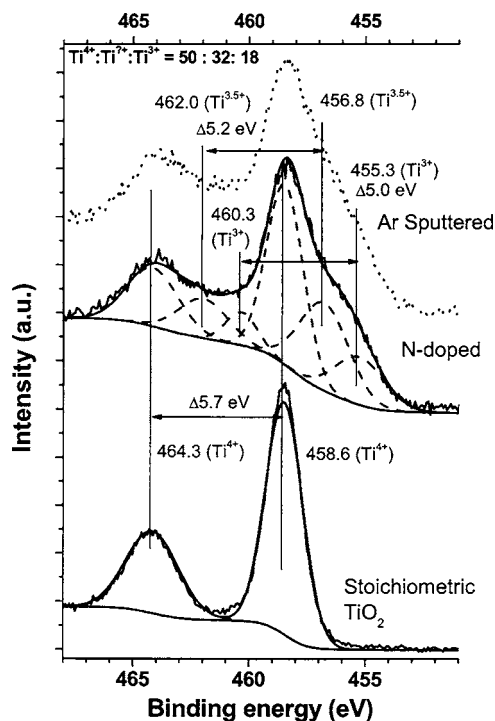


FIG. 1. Ti $2p$ core level spectra for stoichiometric, N-implanted, and Ar⁺ sputtered rutile TiO₂(110), taken all with a photon energy of 625 eV. The spectra at the center and bottom were curve fitted following the procedure described in the text. For the curve fitting, Shirley's background was employed.

purity with respect to N₂(g) formation was determined through

$$E(\text{N}_2 \text{ formation}) = \frac{1}{2}E(\text{gaseous N}_2) + E(\text{perfect surface}) - E(\text{ads-N or int-N}). \quad (5)$$

III. RESULTS

A. Photoemission experiments

Figure 1 shows Ti $2p$ core level spectra for stoichiometric, N-implanted, and Ar⁺ sputtered TiO₂(110). The Ti $2p$ spectrum of TiO₂ reduced by Ar⁺ bombardment is quite similar to that of N-implanted TiO₂. The Gaussian curve fitting of stoichiometric TiO₂ consists of just one pair of peaks. The $2p_{3/2}$ binding energy (BE) of 458.6 eV and the spacing between those peaks of 5.7 eV are consistent with the reported values for Ti⁴⁺ cations in pure TiO₂.^{27,28} On the other hand, the curve fitting of the Ti $2p$ spectrum for N-implanted TiO₂ consists of three doublets. The three lower binding energies (Ti $2p_{3/2}$) are 458.6, 456.8, and 455.3 eV. The first one matches the position for Ti⁴⁺ in TiO₂, and the third one (455.3 eV) is very close to the position reported for bulk TiN (Ti³⁺) (Refs. 29 and 30) or found for Ti³⁺ cations associated with O vacancies in pure titania.^{27,28} There is a report that assigned the second peak (456.8 eV) to Ti⁺ (Ref. 28) induced by the formation of N–Ti–O bonds,³¹ however, as noted above, our Ar⁺-reduced TiO₂ spectra have an almost identical line shape. Thus, the second peak at 456.8 eV cannot be taken as direct evidence for N–Ti–O formation. This second peak was already observed in past Ar⁺ bombardment

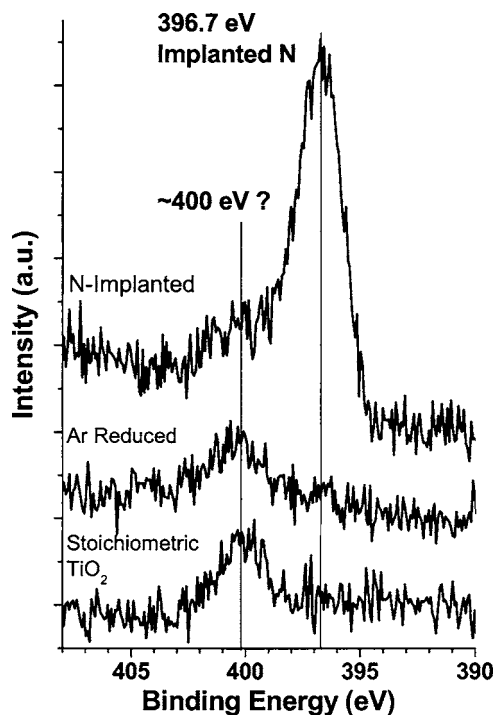


FIG. 2. N $1s$ core level spectra for stoichiometric, Ar⁺ reduced, and N-implanted rutile TiO₂(110), all taken with an excitation energy of 625 eV.

experiments³⁰ and was assigned to Ti³⁺ while the third peak (455.3 eV) was assigned to Ti²⁺; however, these assignments are in conflict with reported TiN results.^{29,30} According to the Perkin Elmer XPS handbook,²⁷ there is no compound reported which shows a Ti $2p_{3/2}$ BE around 457 eV. Even TiO, whose Ti valence must be 2+, shows its BE around 455 eV (Ref. 32) which is near the value of TiN (or Ti³⁺). Thus as a conclusion of our experimental results, the third peak of 455.3 eV is assigned to Ti³⁺ while the second peak of 456.8 eV is assigned to a mixed state of 3+ and 4+. However, these mixed states do not necessarily imply N–Ti–O bonding. The Ti³⁺ cations seen in the Ti $2p$ spectra of Fig. 1 could be in the lattice of titania or in interstitial positions.¹¹ In our study, we did not find evidence for a massive 1×2 reconstruction of the rutile (110) surface.¹¹ Such a reconstruction should produce a much larger Ti³⁺ signal than seen in our photoemission spectra where only one to two layers near the surface are probed. Furthermore, Ti $2p$ spectra obtained for N implantation and Ar⁺ bombardment are almost identical (see top of Fig. 1). Other authors also have not seen a massive 1×2 reconstruction after the implantation of small amounts of N ($\leq 5\%$) in the rutile (110) surface.¹⁶

Figure 2 displays N $1s$ spectra from different TiO₂ surfaces. Even on clean (stoichiometric) TiO₂, a peak centered at ~ 400 eV is observed. This unexpected peak has already been reported by several group in past papers,^{33,34} and assigned to a very minor amount of molecular nitrogen bonded to surface defects. It corresponds to a concentration of less than 1%. Our previous studies for NO and NO₂ adsorption on TiO₂(110) indicate that the 400 eV peak could be the result of bonding N to O sites,¹² a hypothesis that is consistent with the results of the DFT calculations to be shown below. The peak centered at 396.7 eV is observed only in the

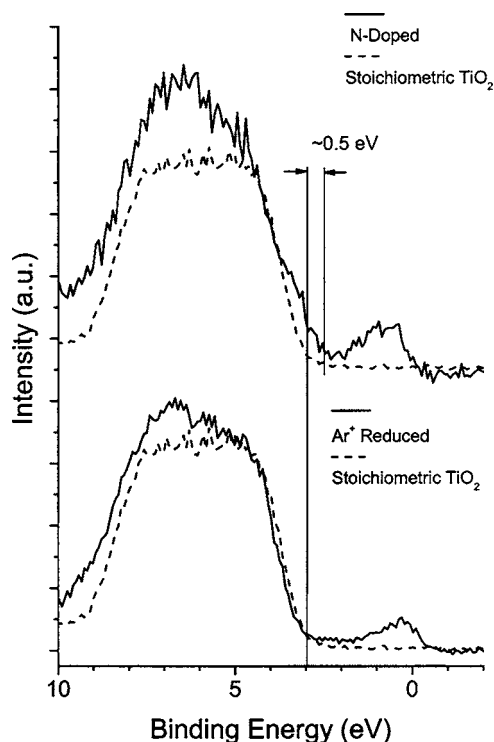


FIG. 3. Valence band spectra for Ar^+ reduced and N-implanted rutile $\text{TiO}_2(110)$, acquired with a photon energy of 325 eV. Dashed lines denote the reference spectrum from stoichiometric $\text{TiO}_2(110)$.

nitrogen implanted sample and naturally attributed to incorporated nitrogen species. Its BE (396.7 eV) is close to the reported BE of TiN ,^{29,31} and this accordance suggests that the implanted nitrogen and titanium make bonds with each other. The amount of implanted nitrogen was estimated by comparing this N 1s peak intensity and O 1s intensity (not shown) considering the calibration of photon flux, photoionization cross section, and electron escape depth. Photon flux was calibrated by the background intensity, and the calibration of photoionization cross section was referred from the literature.³⁵ The electron escape depth was calibrated by calculating the inelastic mean free path (IMFP) of the typical kinetic energy for O 1s and N 1s signals in TiO_2 using the Tanuma-Penn-Powell method (TPP-2M) equation.³⁶ The estimated amount of nitrogen in $\text{TiO}_{2-x}\text{N}_y$ was $y=0.1$ (or $\sim 5\%$). Interestingly, we found that this 5% was the saturation concentration for implanted nitrogen, i.e., it was impossible to increase this nitrogen concentration by longer implantation time or by adding cycles of nitrogen ion implantation.³⁷ Such saturation suggests that the recombination of incorporated nitrogen atoms in TiO_2 and their escape as N_2 from the TiO_2 cage take place when the nitrogen concentration in TiO_2 exceeds a certain value. Previous studies usually found N saturation concentrations of 1–6% depending on the preparation method.^{6,11,15,16} As the density-functional theory (DFT) results will show below, these small concentrations of the dopant are a consequence of the low stability of N in the oxide lattice.

Figure 3 shows valence band spectra excited by soft x-rays (325 eV) from three different TiO_2 samples. The top of the valence band [or highest occupied molecular orbital

(HOMO)] for stoichiometric TiO_2 is around 3 eV in agreement with a previously reported value.³⁸ Also this edge energy can explain well the ultraviolet absorption profile of rutile TiO_2 (3 eV) with the assumption that the lowest unoccupied molecular orbital (LUMO) position is just above the 0 of BE [in order to simplify the discussion, this $\text{BE}=0$ is referred as Fermi energy (E_F) in this paper]. In the two cases of N-implanted and Ar^+ -reduced TiO_2 , there are new states just below E_F and they can be assigned to the occupied 3d states of Ti^{3+} ($[\text{Ar}]3d^1$ configuration versus $[\text{Ar}]3d^0$ configuration in Ti^{4+}).¹² Also, the reported valence band spectrum of TiN ($\text{Ti}^{3+}\text{N}^{3-}$) has similar just below E_F states.³⁰ The line shape for the Ti^{3+} states in the N-implanted and Ar^+ -reduced TiO_2 is somewhat different, with the signal for the N-implanted sample spreading towards higher BE. Thus, the Ti^{3+} states in these samples may not be quite equivalent (Ti-N versus Ti-O bonding). In addition, for the N-implanted TiO_2 , there are extra features above the top of the O 2p band, which shift the edge by ~ 0.5 eV towards E_F . The magnitude of this shift is consistent with the redshift observed in the ultraviolet spectrum of N-doped TiO_2 , where the absorption edge appears at 450 nm (~ 2.7 eV) versus 390 nm (~ 3 eV) for the spectrum of pure TiO_2 .^{6,16,39} Thus, if we assume that the bottom of the conduction band (LUMO) is not affected by the nitrogen implantation, a common assumption,⁸ the redshift observed in the ultraviolet spectrum can be explained by the shift in the top of the valence band seen in Fig. 3 for N-implanted TiO_2 . There is no need to consider transitions from the occupied d states of Ti^{3+} to the conduction band since d-d transitions are usually electric-dipole forbidden (Laporte's rule⁴⁰).

Nitrogen ion implantation led to a change in the chemical properties of the oxide system. This effect is clearly shown in Fig. 4. After the nitrogen ion implantation or argon ion bombardment treatment, the TiO_2 substrates were annealed at 800 K in 1×10^{-6} torr of O_2 for 15 min. This oxygen treatment easily reoxidizes the Ar^+ induced Ti^{3+} to Ti^{4+} , while the N induced Ti^{3+} does not oxidize so much. This results shows that the implanted nitrogen stabilizes the reduced Ti^{3+} species. A recent theoretical study for bulk N-doped anatase indicates that the isolated electron in nitrogen and the excess electron in Ti^{3+} interact and stabilize each other.⁴¹ The DF calculations described below for N-doped rutile $\text{TiO}_2(110)$ show attractive interactions between nitrogen and O vacancies with a N-induced reduction in the energy for the formation of O vacancies. It should also be noted that in the experiments of Fig. 4, annealing at high temperature under O_2 did not result in a significant decrease in the concentration of nitrogen in the sample.

B. Density functional calculations

We investigated the implantation of N in a stoichiometric $\text{TiO}_2(110)$ system or a system containing O vacancies. In principle, the N atoms could replace different types of O atoms in the oxide lattice [see Fig. 5(a)]. The most important positions are bridging (N_{bridg} in our notation), in plane (N_{inp}), and sub-bridging ($\text{N}_{\text{subbridg}}$). The N atoms also could be adsorbed on the surface [Fig. 5(b)], N_s , or be

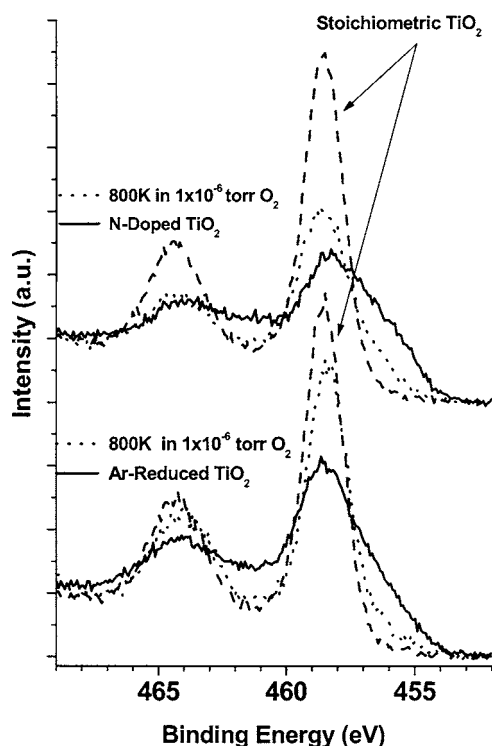


FIG. 4. Ti 2*p* core level spectra recorded before (solid) and after annealing (dotted; 15 min at 800 K, $\sim 10^{-6}$ Torr of O₂) Ar⁺-reduced (bottom) and N-implanted (top) TiO₂(110). For comparison the corresponding results for stoichiometric TiO₂(110) are also included (dashed traces).

trapped inside the channels of the crystal structure [Fig. 5(c)], N_{ch} . As we will see at the end of this section, coadsorption with O vacancies affects the stability of N in all these situations. The relevant positions for the O vacancies are bridging (V_{bridg} in our notation), in plane (V_{inp}), sub-bridging (V_{subbridg}), and in plane2 (V_{inp2}). Our models are for a nonreconstructed surface,^{16,33} since we saw no evidence for a (1×2) reconstruction¹¹ or something similar. We also did not include Ti³⁺ cations in interstitial positions in our models, since the structural geometry for such species is not well known. Studies of synchrotron-based x-ray diffraction and x-ray-absorption fine structure (XAFS) for N-doped titania powders (1%–5% N concentration) show only the typical lattice of the oxide (i.e., no extra phases), with nitrogen as part of the crystal structure or inside the channels, and no evidence for interstitial Ti³⁺ cations.¹⁵ Our models do allow for the interaction of Ti³⁺ sites in the oxide lattice and the implanted N.

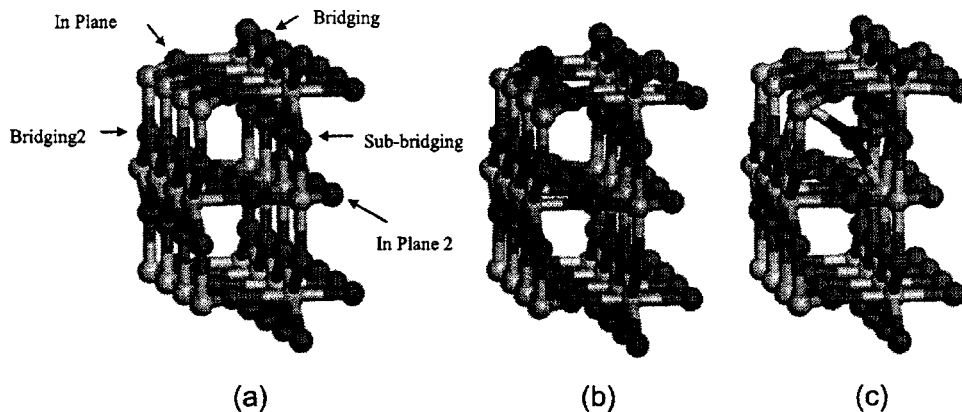


FIG. 5. (a) Substitutional and vacancy site nomenclatures. Exothermic adsorption sites for N(*g*) on the nondefective TiO₂(110) surface: (b) pseudohollow and (c) interstitial in the channel. Code of colors: N (black or blue in the web), O (dark gray or red in the web), and Ti (gray).

TABLE I. Relative energies (eV) for structural N substitution and oxygen vacancies in different positions of TiO₂(110). See Fig. 5(a) for an explanation of our nomenclature. N_{imp} refers to implanted nitrogen and V_{O} denotes an oxygen vacancy.

Positions	$\Delta E(N_{\text{imp}})$	$\Delta E(V_{\text{O}})$
Bridging	0.62	0.00
Sub-bridging	0.31	0.58
In plane	0.10	2.13
In plane2 (bulk)	0.00	>2.3

1. Adsorption and implantation of atomic N in rutile TiO₂(110)

On a stoichiometric rutile TiO₂(110) surface, the only stable sites for the adsorption of atomic N are the pseudohollow (Ti–O–Ti) position [Fig. 5(b)] on the surface, with a N adsorption energy of -1.57 eV, and an interstitial site in the channel [Fig. 5(c)], with an adsorption energy of -1.05 eV. The Ti atop position on the surface is a nonbonding site for a nitrogen atom with an adsorption energy of 0.23 eV. On the other hand, we have studied the substitutional sites. The relative energies of the different substitutional positions for N [Fig. 5(a)] are given in Table I, $\Delta E(N_{\text{imp}})$. The most stable positions are the “in-plane” ones. The order of stability is in plane (bulk) > in plane (surface) > sub-bridging > bridging.

The photoemission spectra in Figs. 1 and 3 indicate the coexistence of implanted N atoms and O vacancies. For a rutile TiO₂(110) surface, we have considered the stability of the oxygen vacancies in different positions [see Fig. 5(a)]. Their relative formation energies, $\Delta E(V_{\text{O}})$, are given in Table I. The order of stability is just the opposite to that of substitutional N: bridging > sub-bridging \gg in-plane positions. This seems to imply that the oxygen vacancies have a tendency to be in the surface while the substitutional nitrogens have a tendency to go to the bulk. Of course, a migration process inside the oxide lattice could be hampered by significant activation barriers and one could have metastable states with N near the surface and O vacancies trapped in the bulk. Also, Ti³⁺ cations may be coupled with the movement of the O vacancies.¹¹

The N adsorption energies on O vacancies located at bridging and sub-bridging sites are -1.72 and -2.71 eV, respectively. We also considered the reaction of atomic nitrogen adsorbed on the surface (N_{s}) with the vacancy sites. The covering of an O vacancy at a bridge position by a N adatom

TABLE II. Calculated energies for the formation of $N_2(g)$ and an oxygen vacancy from structural N implanted in $TiO_2(110)$ surface.

$TiO_{2-x}N_x \rightarrow TiO_{2-x} + x\frac{1}{2}N_2$	ΔE (eV)
Bridging	-3.26
Sub-bridging	-2.38
In plane	-0.61

releases -0.2 eV. The released energy is larger if the O vacancy is at an in-plane position ($\Delta E = -2.8$ eV). Interstitial nitrogen in the channel (N_{ch}) also likes to cover the oxygen vacancy sites. In these cases, the liberated energies are -3.3 eV (O vacancy in plane) and -1.6 eV (O vacancy sub-bridging). Thus, the adsorbed and interstitial N atoms have a tendency to bond to oxygen vacancy sites. Oxygen vacancies will survive in N-implanted $TiO_2(110)$ only if they have a higher concentration than the expected concentration of nitrogen ($TiO_{2-x}N_y$, $x > y$).

2. Recombination of N atoms to form N_2 and oxygen vacancies

Two N_s can move on the surface and meet. The energy liberated in the formation and desorption of N_2 would be -6.8 eV. A similar amount of energy is liberated in the coupling of adsorbed N_s and substitutional N_{bridg} to form $N_2(g)$ and an O vacancy at a bridging position: -6.7 eV. Another possible meeting of N atoms on the surface is an adsorbed N_s with a substitutional N_{inp} to form $N_2(g)$ and an O vacancy at an in-plane position (V_{inp}). That process releases -4.0 eV. The last possibility we considered was the formation of $N_2(g)$ and two V_{inp} from the union of two N_{inp} . The overall reaction is still exothermic ($\Delta E = -1.2$ eV) but we believe that this process is less likely due to the energetic barriers that have to be overcome to pull out two N_{inp} at the same time. In any event, such a process would be possible at high temperature when the motion of the atoms in the surface layer is high. We conclude that the vacancies of the surface layer will not be covered with N at a high concentration of nitrogen impurities because the N atoms initially placed at vacancy sites will eventually be removed by recombination with other N (see Table II).

N atoms trapped inside the channels of titania during implantation can also react with substitutional N atoms to form N_2 . One possibility is the union of an interstitial nitrogen adsorbed in the channel (N_{ch}) with a nitrogen in the surface layer (N_{inp}) to form $N_2(g)$ and V_{inp} ($\Delta E = -4.5$ eV). This means that V_{inp} and N_{inp} are like exit doors for N atoms trapped in the channel (N_{ch}). Another favored process is the union of two N_{ch} to form N_2 trapped or adsorbed in the channel ($\Delta E = -1.7$ eV). The encounter of a N_{ch} with $N_{subbridg}$ to form N_2 trapped in the channel and $V_{subbridg}$ is a less favored process ($\Delta E = -0.2$ eV). In general we found that N atoms embedded in the bulk of titania are metastable sites. They will recombine and may be trapped as N_2 in the oxide channels, but eventually will go into the gas phase at high temperature. This theoretical prediction is consistent with N *K*-edge x-ray appearance near-edge structure (XANES) measurements for N-doped $TiO_2(110)$.³⁷ At room temperature,

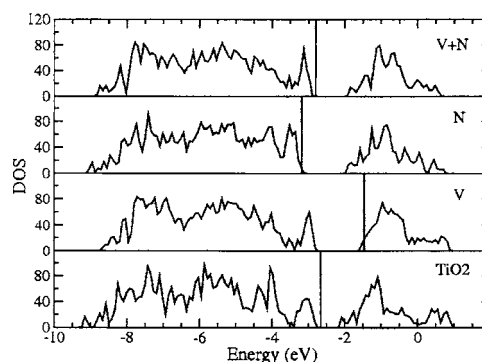


FIG. 6. Density of states (DOS) for a series of systems. A nondefective $TiO_2(110)$ surface is indicated with the label “ TiO_2 ,” the presence of a bridging vacancy is indicated by V, the presence of a structural N impurity in a plane position is indicated by “N,” the presence of both together is indicated by V+N. The highest occupied level is indicated by a vertical line.

only the signal of atomic N is seen near the sample surface, but for the bulk clear peaks of molecular N_2 are detected.³⁷ The trapped N_2 eventually desorbs when the sample is heated from 300 to 600 K.

The instability of implanted N with respect to formation of $N_2(g)$ and vacancies in the surface is due to the strong N–N bond in the molecule. We have calculated the formation energy of the N_2 molecule to check that we are not overestimating the strength of the N–N bond. Our calculated formation energy of N_2 from two N atoms is -9.96 eV which is in very good agreement with the experimental value (-9.80 eV).⁴² Thus, the instability of implanted N with respect to $N_2(g)$ formation is not an artefact of our calculations. In order to keep the N inside the TiO_2 lattice, one has to maintain a low concentration of the dopant to minimize N–N interactions.

3. Electronic interaction between N impurities and oxygen vacancies

The photoemission results in Fig. 4 point to a strong interaction between N impurities and oxygen vacancies. We have examined this issue using DF calculations. These major findings are (i) when a nitrogen atom is present in the surface the formation energy of a bridging O vacancy falls from 2.13 eV (on a nondefective surface) to 0.6 eV and (ii) when a V_{bridg} and a N_{inp} are present together the energy to form $N_2(g)$ and leave a second O vacancy grows from -0.61 to 1.3 eV. These results indicate that the presence of N impurities in the surface favors the formation of O vacancies and the presence of vacancies in the surface stabilizes the N impurities with respect to $N_2(g)$ formation. In practical terms, to generate a very stable N species during the implantation process one needs two O vacancies in the titania lattice. The first one to accommodate the N atom and the second one to stabilize it. In the photoemission results of Figs. 1–4, the implanted N stable at high temperature always coexisted with a substantial amount of O vacancies.

We have performed a study of the density of states to determine the changes in the electronic structure of the system when implanted N and O vacancies coexist. Plots for the density of states of four different systems are shown in Fig. 6: a nondefective and pure surface, a surface with a V_{bridg} , a

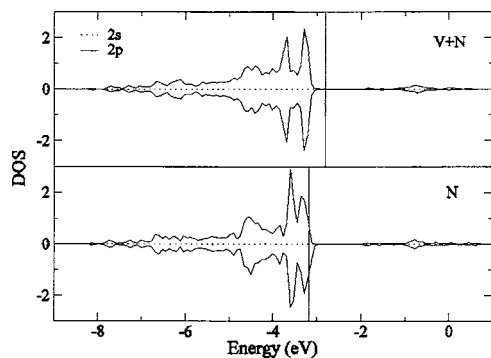


FIG. 7. Representation of the $2p$ band from the DOS projected on a N atom. Alpha states are represented by positive values and beta states are negative values. The label N indicates the presence of a N “in-plane” impurity. The label N+V indicates the presence of both a N in-plane impurity and a bridging O vacancy in the system. The highest occupied level is indicated by a vertical line.

surface with a N_{inp} impurity, and a surface with V_{bridg} and N_{inp} together. The nondefective and pure TiO₂ surface (bottom panel) shows a full O $2p$ band and an empty Ti $3d$ band which is expected for a stoichiometric TiO₂ system where the formal oxidation state for O is -2 and $+4$ for Ti. When an O vacancy is present new states are occupied in the $3d$ band (second panel from bottom). This means that the departed oxygen atom leaves two electrons in the system which are mainly going to two Ti⁴⁺ ions to form two Ti³⁺ ions. When an oxygen atom in the surface is replaced by a N impurity new empty states appear at the top of the O $2p$ band (third panel from bottom). This indicates that the N atom has a formal oxidation state of -2 and its $2p$ orbitals are not fully occupied. If this is true, that nitrogen atom must have a doublet spin state. We have checked this question projecting the density of states on the N atom (Fig. 7, bottom). Indeed, it can be seen that N has empty states in the $2p$ band and has spin polarization since the alpha and beta states are not symmetric and actually do not integrate to the same value. If the O vacancies produce occupation in the higher energy $3d$ band and N impurities produce empty states in the lower energy $2p$ band, when they are together the electrons should go from occupied $3d$ states (Ti³⁺) to lower energy empty $2p$ states (N²⁻ impurities). This electron transfer makes a N²⁻ ion (doublet) change to a N³⁻ ion filling the $2p$ band (singlet). If this is true, the spin polarization of the N impurities should have disappeared and its $2p$ orbitals should be filled. Figure 7 (top) shows the projection of the density of states on that N which has a neighbor V_{bridg} . Its alpha and beta states are full and they are symmetric. These conclusions about the interaction of N impurities with oxygen vacancies are in good agreement with electron paramagnetic resonance (EPR) spectra,⁴¹ in which it is seen that N impurities produce spin polarization but when the system is annealed these states start to disappear. The electrons are pumped from the O vacancies to the N impurities and they are filling the N electronic shells.

This electron transfer mechanism explains the two effects showed above: the lowering of the formation energy of an oxygen vacancy and the stabilization of the N impurities with respect to N₂(g) formation. The N impurity is stabilized

because its shell is closed with the electron transfer from the O vacancy. The energy required for the O vacancy formation is less because one electron left by the leaving oxygen is stabilized by being pumped to close the open shell of the N. Furthermore, in the presence of embedded N there is an extra hybridization of the Ti $3d$ orbitals with the O and N $2p$ orbitals that creates additional states which overlap with the O $2p$ band of TiO₂. One of the two electrons associated with an O vacancy goes to these stable hybrid states and the other goes to a N impurity.

As a final remark, we point out the relation between the photocatalytic decomposition of water and the nitrogen implantation effects. It is obvious that the perturbation in the electronic properties of the valence band enhances the efficiency for absorption of visible light. Furthermore, the stabilization of the reduced Ti state also can add an important property to the TiO₂ surface for the evolution of hydrogen. Prior to the photoinduced hydrogen/oxygen formation ($2\text{H}^+ + 2e \rightarrow \text{H}_2$; $4\text{OH}^- + 4h \rightarrow 2\text{H}_2\text{O} + \text{O}_2$), the ionic water dissociation ($\text{H}_2\text{O} \rightarrow \text{H}^+ + \text{OH}^-$) must take place on the surface, and Henderson has pointed out that this reaction hardly takes place without a surface defect site (Ti³⁺ state).⁴³ Namely, on the defect-free TiO₂(110) ionic dissociation of water is very difficult so that hydrogen/oxygen formation never takes place. This means that not only the redshift in the valence band but also the stabilization of reduced Ti can be playing an important role in the hydrogen/oxygen synthesis reaction on this photocatalytic system.

IV. SUMMARY AND CONCLUSIONS

The electronic properties of N-doped rutile TiO₂(110) have been investigated using synchrotron-based photoemission and density-functional calculations. The doping via N₂⁺ ion bombardment leads to the implantation of N atoms that coexist with O vacancies. Ti $2p$ core level spectra show the formation of Ti³⁺ and a second partially reduced Ti species with oxidation states between $+4$ and $+3$. The valence region of the TiO_{2-x}N_y(110) systems exhibits a broad peak for Ti³⁺ near the Fermi level and N-induced features above the O $2p$ valence band that shift the edge up by ~ 0.5 eV. The magnitude of this shift is consistent with the redshift observed in the ultraviolet spectrum of N-doped TiO₂.

The maximum concentration of N implanted in rutile TiO₂(110) is $\sim 5\%$. The implanted N atoms have a tendency to recombine and form N₂(g) leaving behind oxygen vacancies. This process can be avoided at very low concentrations of N or when the oxide has a substantially large concentration of vacancies. The experimental and theoretical results show the existence of attractive interactions between the dopant and the O vacancies. First, the presence of N embedded in the surface layer reduces the formation energy of O vacancies. Second, the existence of O vacancies stabilizes the N impurities with respect to N₂(g) formation. When oxygen vacancies and N impurities are together there is an electron transfer from the higher energy $3d$ band of Ti³⁺ to the lower energy $2p$ band of the N²⁻ impurities.

ACKNOWLEDGMENTS

The research done at the Chemistry Department of Brookhaven National Laboratory was financed through Contract No. DE-AC02-98CH10086 with the U.S. Department of Energy (DOE), Division of Chemical Sciences and by BNL LDRD funding. The NSLS is supported by the Divisions of Chemical and Materials Sciences of U.S. DOE. Financial support from the Spanish *Ministerio de Ciencia y Tecnología* (MAT2005-01872) and the Junta de Andalucía (FQM-132) is appreciated by the two of the authors (J.G.) and (J.F.S.)

- ¹A. Fujishima and K. Honda, *Nature* (London) **238**, 37 (1972).
- ²M. Grätzel, *Nature* (London) **414**, 338 (2001).
- ³H. Arakawa and K. Sayama, *Catal. Surv. Jpn.* **4**, 75 (2000).
- ⁴J. M. Bolts and M. S. Wrighton, *J. Phys. Chem.* **80**, 2641 (1976).
- ⁵K. Domen, A. Kudo, and H. Onishi, *J. Catal.* **102**, 92 (1986).
- ⁶R. Asahi, T. Morikawa, T. Ohwaki, K. Aoki, and Y. Taga, *Science* **293**, 269 (2001).
- ⁷X. Chen and C. Burda, *J. Phys. Chem. B* **108**, 15446 (2004); M. Sathish, B. Viswanathan, R. P. Viswanath, and C. S. Gopinath, *Chem. Mater.* **17**, 6349 (2005); G. R. Torres, T. Lindgren, J. Lu, C.-G. Granqvist, and S.-E. Linquist, *J. Phys. Chem. B* **108**, 5995 (2004); C. Belver, R. Bellod, S. J. Stewart, F. G. Requejo, and M. Fernández-García, *Appl. Catal., B* **65**, 309 (2006).
- ⁸R. Nakamura, T. Tanaka, and Y. Nakato, *J. Phys. Chem. B* **108**, 10617 (2004); M. Mrowetz, W. Balcerski, A. J. Colussi, and M. R. Hoffmann, *ibid.* **108**, 17269 (2004).
- ⁹C. Di Valentin, G. Pacchioni, and A. Selloni, *Phys. Rev. B* **70**, 085116 (2004).
- ¹⁰J. Y. Lee, J. Park, and J.-H. Cho, *Appl. Phys. Lett.* **87**, 011904 (2005).
- ¹¹M. Batzill, E. Morales, and U. Diebold, *Phys. Rev. Lett.* **96**, 026103 (2006).
- ¹²J. A. Rodriguez, T. Jirsak, G. Liu, J. Hrbek, J. Dvorak, and A. Maiti, *J. Am. Chem. Soc.* **123**, 9597 (2001).
- ¹³J. L. Gole, J. D. Stout, C. Burda, Y. Lou, and X. Chen, *J. Phys. Chem. B* **108**, 1230 (2004).
- ¹⁴H. Li, J. Li, and Y. Huo, *J. Phys. Chem. B* **110**, 1559 (2006).
- ¹⁵H. Chen, W. Wen, A. Nambu, J. Graciani Alonso, J. Hanson, J. A. Rodriguez, and E. Fujita (unpublished).
- ¹⁶O. Diwald, T. L. Thompson, T. Zubkov, E. G. Goranski, S. D. Walck, and J. T. Yates, *J. Phys. Chem. B* **108**, 6004 (2004).
- ¹⁷G. Kresse and J. Hafner, *Phys. Rev. B* **47**, R558 (1993).
- ¹⁸G. Kresse and J. Furthmuller, *Comput. Mater. Sci.* **6**, 15 (1996); *Phys. Rev. B* **54**, 11169 (1996).
- ¹⁹D. Vanderbilt, *Phys. Rev. B* **41**, 7892 (1990).
- ²⁰J. Perdew, J. Chevary, S. Vosko, K. Jackson, M. Pederson, D. Singh, and C. Fiolhais, *Phys. Rev. B* **46**, 6671 (1992).
- ²¹H. J. Monkhorst and J. D. Pack, *Phys. Rev. B* **12**, 5188 (1976).
- ²²A. De Vita, Ph.D. thesis, Keele University, 1992; A. De Vita and M. J. Gillan (unpublished).
- ²³J. Harris, *Phys. Rev. B* **31**, 1770 (1985); W. M. C. Foulkes and R. Haydock, *ibid.* **39**, 12520 (1989).
- ²⁴L. Giordano, G. Pacchioni, T. Bredow, and J. F. Sanz, *Surf. Sci.* **471**, 21 (2001).
- ²⁵N. López and J. K. Norskov, *Surf. Sci.* **515**, 175 (2002).
- ²⁶J. Oviedo, M. A. San Miguel, and J. F. Sanz, *J. Chem. Phys.* **121**, 7427 (2004).
- ²⁷*Handbook of X-Ray Photoelectron Spectroscopy*, edited by G. E. Muilenberg (Perkin Elmer Corporation, Eden Prairie, MN, 1979).
- ²⁸A. R. González-Elipe, G. Munuera, J. S. Espinos, and J. M. Sanz, *Surf. Sci.* **220**, 368 (1989).
- ²⁹N. Saha and G. Tompkins, *J. Appl. Phys.* **72**, 3072 (1992).
- ³⁰H. Höchst, R. D. Bringans, P. Steiner, and Th. Wolf, *Phys. Rev. B* **25**, 7183 (1982).
- ³¹F. Esaka, K. Furuya, H. Shimada, M. Imamura, N. Matsubayashi, H. Sato, A. Nishijima, A. Kawana, H. Ichimura, and T. Kikuchi, *J. Vac. Sci. Technol. A* **15**, 2521 (1997).
- ³²H. F. Franzen, M. X. Umaña, J. R. McCreary, and R. J. Thorn, *J. Solid State Chem.* **18**, 363 (1976).
- ³³O. Diwald, T. L. Thompson, E. G. Goranski, S. D. Walck, and J. T. Yates, *J. Phys. Chem. B* **108**, 52 (2004).
- ³⁴H. Irie, S. Washizuka, N. Yoshino, and K. Hashimoto, *Chem. Commun. (Cambridge)* **2003**, 1298.
- ³⁵J. J. Yeh and I. Lindau, *At. Data Nucl. Data Tables* **32**, 1 (1985).
- ³⁶S. Tanuma, C. J. Powell, and D. R. Penn, *Surf. Interface Anal.* **17**, 911 (1991); **21**, 165 (1993); A. Jablonski and C. J. Powell, *J. Electron Spectrosc. Relat. Phenom.* **100**, 137 (1999).
- ³⁷A. Nambu, J. A. Rodriguez, and E. Fujita (in preparation).
- ³⁸S. Bourgeois, B. Domenichini, Z. Li, and P. J. Møller, *Appl. Surf. Sci.* **244**, 399 (2005).
- ³⁹Z. Lin, A. Orlov, R. M. Lambert, and M. C. Payne, *J. Phys. Chem. B* **109**, 20948 (2005).
- ⁴⁰O. Laporte, *Z. Phys.* **23**, 135 (1924).
- ⁴¹C. Di Valentin, G. Pacchioni, A. Selloni, S. Livraghi, and E. Giamello, *J. Phys. Chem. B* **109**, 11414 (2005).
- ⁴²*CRC Handbook of Chemistry and Physics, Internet Version 2005*, edited by D. R. Lide (CRC, Boca Raton, FL, 2005), <http://www.hbcpnetbase.com>.
- ⁴³M. A. Henderson, J. M. White, H. Uetsuka, and H. Onishi, *J. Am. Chem. Soc.* **125**, 14974 (2003).